A large difference between the jet and stream densities raises the question whether or not buoyancy could have introduced errors into the measurements, but a simple estimate[1] showed that this error is insignificant for the present experiments.

The present results have been obtained for a single slot width. The experiments by Vranos and Nolan[2] with circumferential slots (infinite aspect ratio) varying in width between 0.045 and 0.14 in. did not indicate any influence of the slot width on their correlation. For elliptic jets of small aspect ratio (up to 4), they found that the best reference value for w is the diameter of a circle having the same cross-sectional area as the jet (rather than the hydraulic diameter). The correlation thus depends on the aspect ratio of the jet. For circular jets, they observed no effect of jet diameter when the latter was reduced by factors of 1.4 and 2. Ivanov[5] and Shandorov[6] also found no effect of jet size for circular jets when the diameter was increased by about 50%. Similarly, Callaghan, Ruggeri, and Bowden[4] found no effect of jet size for elliptic jets (aspect ratio of 4) when the equivalent jet diameter was reduced by a factor 0.6. Therefore, Eq. (1) or (2) should be satisfactory for some range of the slot width as long as the aspect ratio remains sufficiently large. For the correlation of penetration data for narrow slots (high aspect ratio), the slot width appears to be the appropriate reference dimension. Since the best reference dimension for jets with small aspect ratios is the diameter of a circle having the same cross-sectional area, the appropriate reference dimension must be a function of the jet aspect ratio. Because of its practical importance, this relationship should be sought in future work.

References

[1] Rudinger, G., "Experimental Investigation of Gas Injection Through a Transverse Slot into a Subsonic Cross Flow," Rept. 9500-920288, July 1973, Bell Aerospace Co., Buffalo, N.Y.

[2] Vranos, A. and Nolan, J. J., "Supersonic Mixing of Helium and Air (Unclassified)," *Minutes of 31st Meeting of Bumblebee Propulsion Panel*, Vol. 2, JHU/APL (Confidential), TG 63-53, June 1964, Applied Physics Lab., Silver Springs, Md., pp. 131–161 (Declassified Dec. 31, 1972, Executive Order 11652).

[3] Callaghan, E. E. and Ruggeri, R. S., "Investigation of an Air Jet Directed Perpendicularly to an Air Stream," TN 1615, 1948, NACA.

[4] Ruggeri, R. S., Callaghan, E. E., and Bowden, D. T., "Penetration of Air Jets Issuing from Circular, Square, and Elliptic Orifices Directed Perpendicularly to an Air Stream," TN 2019, 1950, NACA.

[5] Ivanov, Yu.V., "Equation for Trajectories of Jets with Acute Blast" (in Russian), *Sovietskoe Kotloturbostroenie*, Vol. 8, 1952 (quoted in Refs. 2 and 12).

[6] Shandorov, G. S., "Flow from a Channel into Stationary and Moving Media," *Zhurnal Tekhnicheskoi Fiziki*, Vol. 37, 1957, p. 1 (quoted in Refs. 12 and 13).

[7] Keffer, J. F. and Baines, W. D., "The Round Turbulent Jet in a Cross-Wind," *Journal of Fluid Mechanics*, Vol. 15, No. 4, 1963, pp. 481–497.

[8] Endo, H. and Nakamura, M., "Bending and Development of a Three-Dimensional Turbulent Jet in a Cross-Wind" (in Japanese), NAL, TR 216, 1968, National Aeronautical Lab. (quoted in Ref. 14).

[9] Gertsberg, M. B., "Trajectory of Gas Jets Injected into a Subsonic Flow" (in Russian), *Izvestia vyssikh uchebnykh zavedenii aviatsionnaya*, No. 2, 1970, pp. 99–103 (quoted in Ref. 14).

[10] Wu, J. C., McMahon, H. M., Mosher, D. K., and Wright, M. A., "Experimental and Analytical Investigations of Jets Exhausting into a Deflecting Stream," *Journal of Aircraft*, Vol. 7, No. 1, Jan.–Feb. 1970, pp. 44–51.

[11] Kamotani, Y. and Greber, I., "Experiments on a Turbulent Jet in a Cross Flow," *AIAA Journal*, Vol. 10, No. 11, Nov. 1972, pp. 1425–1429.

[12] Abramovich, G. N., *The Theory of Turbulent Jets* (translation from the Russian), MIT Press, Cambridge, Mass., 1963, Sec. 12.4.

[13] Skifstad, J. G., "Aerodynamics of Jets Pertinent to VTOL Aircraft," *Journal of Aircraft*, Vol. 7, No. 3, May–June 1970, pp. 193–204.

[14] LeGrivès, É. and Benoit, A., "A New Theoretical Model for Representing Jet Penetration into a Subsonic Stream" (in French), *La Recherche Aérospatiale*, No. 3, 1972, pp. 133–142.

[15] Hurn, A. G. and Akers, G. A., "Notes on the Effect of a Jet Emerging from a Surface in the Presence of a Mainstream Flow," TN 5, 1955, Boulton Paul Aircraft, Ltd., Wolverhampton, England (quoted in Ref. 13).

Comparison of Calculated Static and Dynamic Collapse Pressures for Clamped Spherical Domes

MARK HARTZMAN*

Lawrence Livermore Laboratory, University of California, Livermore, Calif.

Introduction

THIS Note compares the results of static and dynamic analyses of steel pressure domes used in certain applications at Lawrence Livermore Lab. Figure 1 shows a typical spherical dome that has been built into a thick pipe; the thickness of the dome varies, but a uniform surface loading is applied on the convex surface. The mode of failure of such domes is by sudden collapse—a highly nonlinear problem involving large deformation, large displacements, and elastic-plastic flow.

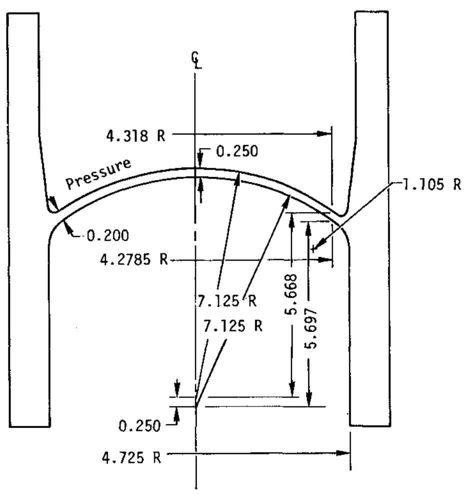

Fig. 1 Dome with pressure on the convex side. All dimensions are in inches.

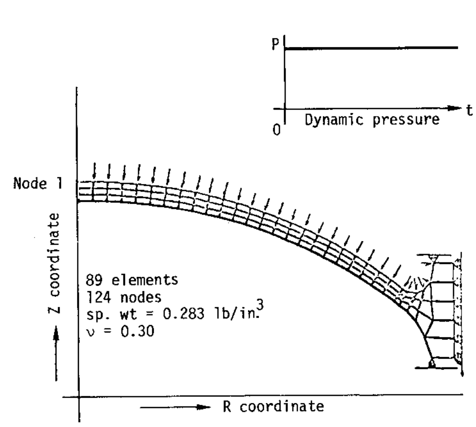

Fig. 2 Finite element model.

Received October 11, 1973. Work performed under the auspices of the U.S. Atomic Energy Commission. The author wishes to thank R. Murray for generating the finite element models.

Index categories: Structural Dynamic Analysis; Structural Stability Analysis; Structural Static Analysis.

* Staff Member, Nuclear Test Engineering Division.

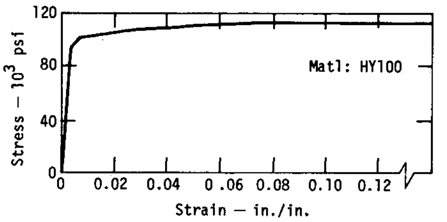

Fig. 3 Engineering uniaxial stress-strain curve.

Analysis

Analysis was performed by applying two finite element nonlinear computer programs: EPSOLA[1] and ADYN.[2] EPSOLA was used for the static analysis, ADYN for the dynamic analysis. Both describe the deformation of axisymmetric bodies subjected to axisymmetric loads, and both include material and geometric nonlinearities.

Figure 2 shows the finite element model of the dome and the dynamic loading. Because of the presence of symmetry, only half the cross-section is shown. Figure 3 shows the material properties and the engineering stress-strain curve. Strain rate effects for the dynamic analysis are ignored.

Results

The results of the static analysis are shown in Figs. 4 and 5. Figure 4 shows the deflection of the dome center (node 1) as a function of pressure loading. The pressure at which yielding occurred was determined as 4110 psi. The pressure was then increased to 10,000 psi in 100 increments. We determined that sudden collapse occurred at 6180 psi. At this pressure a sudden increase in central displacement occurred. Figure 5 shows the cross-section of the dome before, during, and after collapse. Note that substantial deformation occurs in the thin rim of the dome.

The results of the dynamic analysis are shown in Figs. 6–8. This analysis was performed by calculating the dynamic deflection of the dome when it was subjected to applied step loads of varying magnitude. Figure 6 shows the peak central deflection as a function of step pressure magnitude. It appears that beyond 8000 psi the dome experiences considerable deflection for all step loads. This pressure is therefore taken as the dynamic collapse pressure. Figure 7 shows the central displacement history at 10,000 psi applied step pressure. Figure 8 shows the cross section of the dome at various times during the collapse process. The stages are seen to be similar to those obtained in the static analysis.

Discussion and Conclusions

A comparison of static and dynamic analyses shows that the former has a lower collapse pressure. The results of other

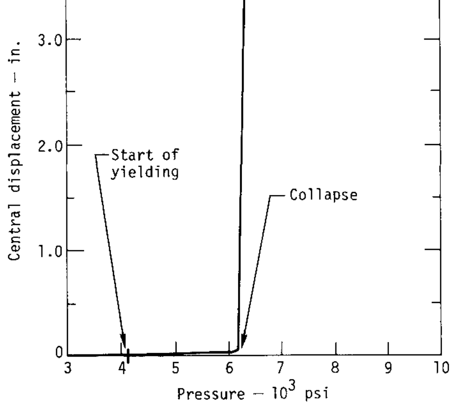

Fig. 4 Displacement of the dome center vs applied static pressure.

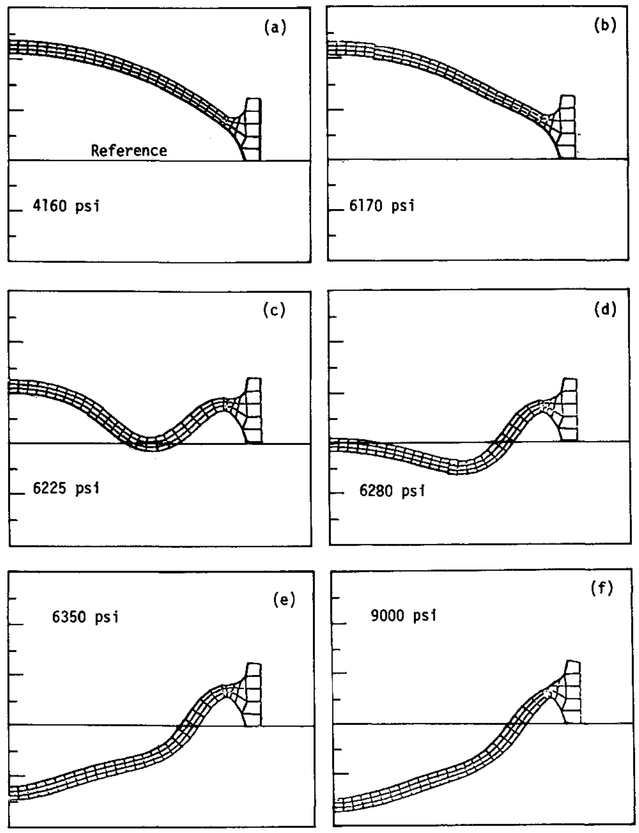

Fig. 5 Stages in dome collapse as a result of static loading.

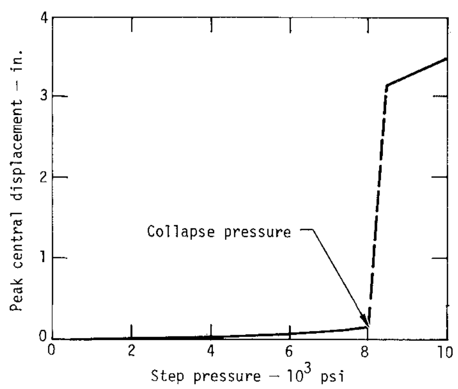

Fig. 6 Peak central deflection vs step pressure magnitude.

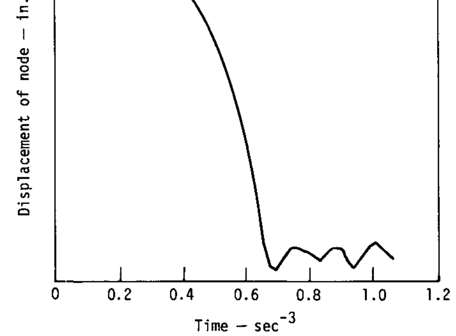

Fig. 7 Central displacement history of the dome under dynamic loading (10,000 psi, step loading).

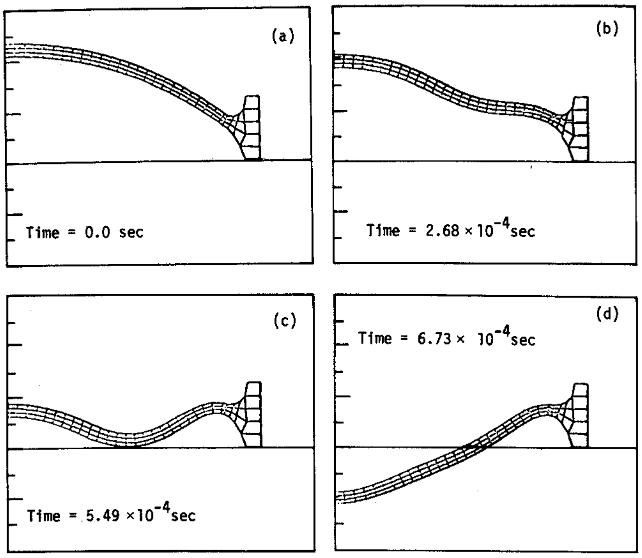

Fig. 8 Stages in dome collapse as a result of dynamic loading (10,000 psi, step loading).

investigators[3,4] indicate a dynamic "weakening" effect for thin, elastic spherical caps, i.e., a lower dynamic collapse or snap through load than static. However, the results of our calculation indicate that for thicker shells, where the material may deform elastic-plastically, it is possible for the dynamic collapse load to be higher than the static. To the author's knowledge no experiments have been performed to determine the collapse behavior of thick spherical shells; such experiments are needed.

References

[1] Hartzman, M., "Static Stress Analysis of Axisymmetric Solids with Material and Geometric Nonlinearities by the Finite Element Method," UCRL-51390, Jan. 1973, Lawrence Livermore Lab., Livermore, Calif.

[2] Hartzman, M., "Nonlinear Dynamic Analysis of Axisymmetric Solids by the Finite Element Method," UCRL-74978, Lawrence Livermore Lab., Livermore, Calif., to be published.

[3] Lock, M. H., Okubo, S., and Whittier, J. S., "Experiments on the Snapping of a Shallow Dome Under a Step Pressure Load," *AIAA Journal*, Vol. 6, No. 7, July 1968, pp. 1320–1326.

[4] Stricklin, J. A. and Martinez, J. E., "Dynamic Buckling of Clamped Spherical Caps under Step Pressure Loading," *AIAA Journal*, Vol. 7, No. 6, June 1969, pp. 1212–1213.

Boundary-Layer Transition on Cones Near Mach One

J. LEITH POTTER*
ARO Inc., Tullahoma, Tenn.

Nomenclature

C_{D_0} = measured drag coefficient corrected to zero angle of attack
M = Mach number
Re = Reynolds number based on wetted length
T = temperature
U/ν = unit Reynolds number
α = angle of attack

Subscripts
p = in plane of photograph
t = at boundary-layer transition
w = wall surface conditions
δ = local edge-of-boundary-layer condition
∞ = freestream condition

SOME data which demonstrate the possibility of using an aeroballistic range for obtaining transition Reynolds numbers near a Mach number of one are presented here. Only a few launches under transonic conditions were made in this program, but the results offer adequate proof of the feasibility of interference-free data when $M_\infty > 1.04$ using 6.4-cm-diam, 10° semiangle sharp cones in 1.8-m-diam Aeroballistics Range K at the AEDC.

The quiet atmosphere of an aeroballistic range appears to offer an opportunity for study of boundary-layer transition free of the complex influences of stream vorticity, entropy spottiness, and noise known to be present in varying degrees in wind tunnels. However, there are some special features of aeroballistic experimentation which raise questions, and it is appropriate that they be reviewed in the context of their potential influence on transition. We refer to the following: 1) finite angles of attack and oscillatory motion, e.g., $\pm 3°$; 2) vibration of the model resulting from launch accelerations; 3) surface roughness under cold-wall conditions at high unit Reynolds numbers; and 4) nonuniform surface temperatures owing to aerodynamic heating.

These have been analyzed in Ref. 1 where it was concluded that there probably is no significant "range-peculiar" influence generated under the conditions of the experiments described in Refs. 1 and 2, and in this Note.

Undeniably, disturbances of some scale may be imposed on the boundary layer because of conditions in the foregoing list, numbers 1 and 2 being of the most concern in the present case. But if one accepts the concept that all real boundary layers suffer disturbances, usually of multiple types, then it is mainly relevant to consider whether these range-peculiar disturbances induce a different transition Reynolds number than that which would result from another set of free-flight circumstances, say free fall through the atmosphere. In other words, we know that wind tunnels impose disturbances on boundary layers of models, we know that a different set of disturbances exists in an aeroballistic range environment, and we know that full-scale free-flight is not disturbance-free either (because of surface conditions, vibration, oscillating motion, etc.). For that reason,

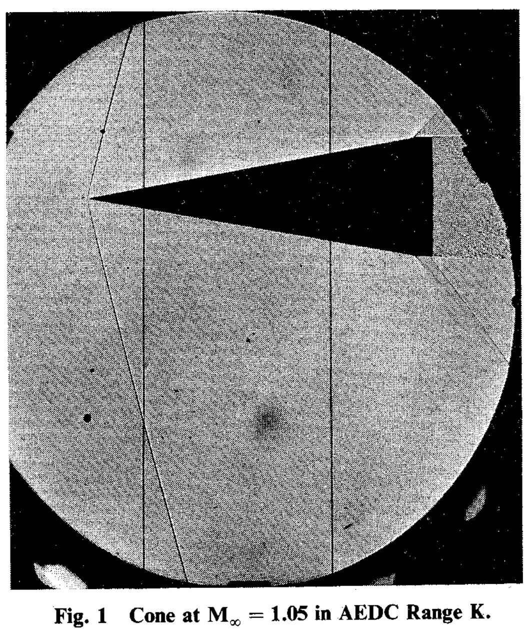

Fig. 1 Cone at $M_\infty = 1.05$ in AEDC Range K.

Received October 17, 1973. Research sponsored by the Arnold Engineering Development Center (AEDC), Air Force Systems Command. Further reproduction is authorized to satisfy needs of U.S. Government. Thanks are owed to E. O. Marchand who computed the inviscid cone surface conditions used in Table 1 and E. E. Callens who assisted with the experiments.

Index categories: Boundary-Layer Stability and Transition; Subsonic and Transonic Flow.

* Deputy Director, von Kármán Gas Dynamics Faculty. Associate Fellow AIAA.